Fabrication of two-component, brush-on-brush topographical microstructures by combination of atom-transfer radical polymerization with polymer end-functionalization and photopatterning

Paul Chapman[1,2], Robert E. Ducker[1], Claire R. Hurley[1, †], Jamie K. Hobbs[2,] and Graham J. Leggett[1,]*.*

Department of Chemistry, University of Sheffield, Brook Hill, Sheffield S3 7HF, UK and Department of Physics and Astronomy, University of Sheffield, Sheffield S3 7RH, UK.

ABSTRACT

Poly(oligoethylene glycol methyl ether methacrylate) (POEGMEMA) brushes, grown from silicon oxide surfaces by surface-initiated atom transfer radical polymerization (SI-ATRP), were end-capped by reaction with sodium azide leading to effective termination of polymerization. Reduction of the terminal azide to an amine, followed by derivatization with the reagent of choice, enabled end-functionalization of the polymers. Reaction with bromoisobutryl bromide yielded a terminal bromine atom that could be used as an initiator for ATRP with a second, contrasting monomer (methacrylic acid). Attachment of a nitrophenyl protecting group to the

amine facilitated photopatterning: when the sample was exposed to UV light through a mask, the amine was deprotected in exposed regions, enabling selective bromination and the growth of a patterned brush by ATRP. Using this approach, micropatterned pH-responsive poly(methacrylic acid) (PMAA) brushes were grown on a protein resistant planar poly(oligoethylene glycol methyl ether methacrylate) (POEGMEMA) brush. Atomic force microscopy analysis by tapping mode and Peak Force quantitative nanomechanical mapping (QNM) mode allowed topographical verification of the spatially specific secondary brush growth and its stimulus-responsiveness. Chemical confirmation of selective polymer growth was achieved by secondary ion mass spectrometry (SIMS).

INTRODUCTION

Polymer brushes (polymer chains grafted onto or grown from solid substrates with a grafting density sufficient to initiate chain stretching away from a random walk conformation) have been widely studied and have found a diversity of applications in surface science and technology[1, 2]. Polymer brushes provide a means to modify the interfacial properties of surfaces, through the selection of appropriate monomers and through control of the architecture of the brush film. For example, brush layers have attracted interest in lubrication systems. By varying the polymer-solvent interactions, the osmotic pressure and hence the coefficient of friction may be controlled[3, 4, 5, 6, 7]; for example, poly(2-(methacryloyloxy)ethyl phosphorylcholine) (PMPC) brushes have been reported to exhibit super-lubricious characteristics[3]. Polymer brushes also find applications in biomedical science. For example, a number of brushes exhibit high resistance to biofouling. Poly(oligoethylene glycol methyl ether methacrylate) (POEGMEMA) bottle-brushes render a variety of surfaces highly resistant to the adsorption of proteins[8, 9, 10, 11]. Other examples

of anti-fouling brushes include polybetaines[12, 13] and poly(amino acid methacrylate) brushes[14, 15, 16].

In many applications, spatial organization of the brush structure is desirable. For example, in the design of biomedical sensors[17, 18, 19] it is often required to be able to organize the adsorption of biomolecules to facilitate the formation of an array. There has been a great deal of interest in the patterning of brush growth. A variety of approaches have been explored, including microcontact printing, photolithography, electron beam lithography and approaches based on scanning probe techniques. Ma and co-authors demonstrated microcontact printing of a thiol based initiator onto a gold substrate for selective brush growth[20]. Direct chemical change by electron beams to allow the spatially selective formation of photoinitiator was utilized by Schmelmer et al[21] and Steenackers et al[22]. Kaholek and co-authors used a scanning probe nano-shaving methodology to remove a background thiol before backfill with a thiol initiator[23].

There has been interest in the fabrication of multiple component polymer patterns, where different components on the surface were designed to elicit contrasting responses. A number of approaches have been utilized in the literature. Low density polymer grafted from a brush was achieved by Brault et al by variation in passivation reaction time and a secondary polymerization[24]. Sequential deposition techniques have been applied, which were based around repeated cycles of patterned initiator deposition by microcontact printing followed by brush growth[25, 26, 27, 28]. This microcontact printing methodology allowed Zhou and co-authors to form binary, tertiary and quaternary patterned brush surfaces[25]. Binary patterned brushes were formed by capillary force lithography using a polystyrene printed mask over a pre-formed initiator layer with polymerization with and without mask[29]. Konradi and Ruhe utilized a masked photopolymerization and secondary thermal polymerization step to form two polymer surfaces[30].

Spatial separation of surface films with different initiator molecules allow multiple types of polymerization to be applied to the same surface[31, 32, 33], such as atom transfer radical polymerization (ATRP) and reversible addition-fragmentation chain-transfer polymerization (RAFT).

Direct patterning methods, such as photolithography, are also attractive. Photo-induced surface-initiated ATRP using an iridium based catalyst has been reported[34, 35]. Spatial control of polymerization is essential for such approaches and in particular, the ability to inhibit further polymerization from previously grafted chains is required if multiple component surfaces are to be formed. The alkyl halide initiator of atom transfer radical polymerization has been shown to undergo nucleophilic substitution with sodium azide to generate an alkyl azide chain terminus in both solution[36, 37, 38] and at a surface[25, 26, 39, 40].

Herein an alternative methodology is reported using reduction of an azide terminated polymer and addition of a photocleavable protecting group. The methodology is displayed in scheme 1. Through selective deprotection, initiation and secondary polymerization, chemically distinct regions and topographic variation were generated from a polymer brush grown on an existing polymer brush surface. The azide reduction scheme has been reported for solution phase polymers[36], however to the best of the authors' knowledge, it has not been applied to surface 'grafted from' polymers. The azide may be converted to an amine, which can be derivatized using nitrophenylpropyloxycarbonyl (NPPOC) protecting groups[41, 42, 43]. These are readily removed, with near-quantitative efficiency, on exposure to near-UV radiation, and have been effectively utilized for surface patterning[44]. Firstly, results for proof of concept experiments on a polymer brush system are presented. Secondly, results for the patterned system using protected

amine-terminated polymer brushes are chracterized by tapping mode atomic force microscopy (AFM), Peak Force QNM AFM and imaging SIMS.

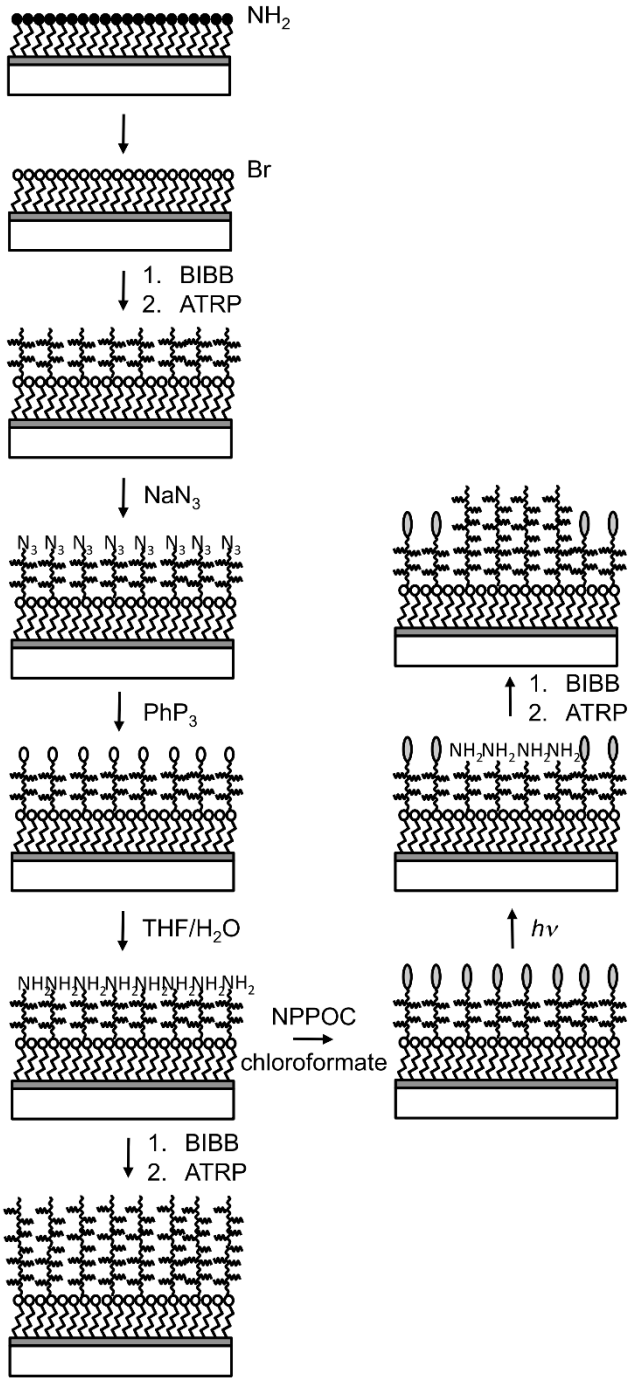

Figure 1. Pictorial representation of the photolithography and reaction scheme for brush formation from a silane film (left top), brush growth from an unpatterned amine-modified brush

surface (left bottom) and patterned brush growth from an amine-modified brush surface (right). Modification reactions occur at the brush chain ends. Straight lines indicate silane film molecules and highly curved lines indicate polymer brush molecules. The diagram is not to scale.

EXPERIMENTAL SECTION

Materials

Silicon wafers (reclaimed, p-type, <100>) were purchased from Compart technology (Peterborough, UK) and glass coverslips (22 mm x 60 mm, thickness 1.5) were supplied by Menzel Gläser. Copper(I) bromide (≥98%), copper(II) bromide (99.999%), 2,2'-bipyridyl (≥99%), poly(ethylene glycol) methyl ether methacrylate (Mn ~ 500), triethylamine (≥99%), α-bromoisobutyryl bromide (98%), (3-aminopropyl)triethoxysilane (≥98%), sodium azide (≥99.5%), triphenylphosphine (99%), 2-(2-nitrophenyl)propyl (NPPOC) chloroformate (95%) and tetrahydrofuran (THF, HPLC grade) were supplied by Sigma-Aldrich (Poole, UK). Sulfuric acid (s.g. 1.83, >95%), hydrogen peroxide (30% v/v), ammonia solution (s.g. 0.88, 35%), ethanol (HPLC grade), toluene (HPLC grade), dichloromethane (HPLC grade) and methanol (HPLC grade) were supplied by Fisher (Loughborough, UK). N,N-dimethylformamide (DMF) was collected from an onsite Grubbs dry solvent system. Deionized water was purified by an Elga PURELAB option to 15 MΩ cm.

Glass slides and silicon wafers in glass tubes were cleaned thoroughly by immersion in piranha solution (30% hydrogen peroxide, 70% concentrated sulfuric acid) for ca. 30 min. Warning! If there are excess organic molecules or solvents in glassware, the addition of piranha can be explosive. Substrates and glass tubes were then rinsed seven times with deionized water. The substrates underwent a further clean with a solution of 70% deionized water, 15% hydrogen peroxide and 15% ammonia solution which was heated and left boiling for 30 minutes. This was

followed by seven repeated rinses in deionized water, after which the substrates were blown dry to remove excess water and placed in a drying oven overnight. To form silane films, they were immersed in a 0.2 M solution of 3-aminopropyl)triethoxysilane (APTES) in toluene for 30 min. The samples were sonicated during the first 5 min of this period. Subsequently, the surfaces were rinsed with toluene, ethanol/toluene (1:1), and then ethanol and blown dry with nitrogen. Samples were placed in a vacuum oven within foil wrapped glass tubes for 20 min at 120°C.

Prior to carrying out atom-transfer radical polymerization, APTES-treated substrates were immersed in a solution of 0.4 M triethylamine and 0.4 M α-bromoisobutyryl bromide in dichloromethane for 60 min. Samples were rinsed thoroughly with dichloromethane and then ethanol and dried with nitrogen before polymerization.

Azide reactions

Sodium azide was placed in a round bottomed flask before dry dimethylformamide, which was degassed with nitrogen for 20 min, was added to give a 0.2 M solution. After mixing and further degas, the saturated solution was added to substrates in carousel tubes under nitrogen which were then heated at 60°C for 18 h.

Triphenylphosphine was placed in a round bottomed flask before dry dimethylformamide, which was degassed for 20 min, was added to give a 0.2 M solution. After further degas, the solution was added to substrates in carousel tubes under nitrogen and heated at 60°C for 18 h. Substrates were rinsed with DMF, water and ethanol, blown dry with nitrogen and returned to a carousel tube. Water and tetrahydrofuran were mixed well before addition to the carousel tubes under nitrogen, which were then heated at 40°C for 18 h.

Polymerization reactions

Initiated substrates were loaded into carousel tubes, sealed, underwent three vacuum-nitrogen cycles, and kept under nitrogen. In a round bottom flask, 4 mL of degassed water and 16 mL of methanol was added to 20 mL poly(ethylene glycol) methyl ether methacrylate monomer (OEGMEMA). The flask was degassed for 30 min, before 0.37 g copper(I) bromide and 0.81 g 2,2'-bipyridyl were added. After being sufficiently mixed and degassed, approximately 1 to 2 mL of monomer-catalyst solution was added to the carousel tube to cover each substrate. Once polymerization time had elapsed, the substrate was thoroughly sonicated in water, rinsed with water and ethanol, and blown dry with nitrogen.

A similar procedure was used to polymerize methacrylic acid, however pre-mixing of the catalyst was required due to potential coordination of the monomer and copper in this case. The monomer (10 mL) was adjusted to pH 9 with 20 mL 6 M NaOH (aq). In a second flask, 10 mL of water was added. Both flasks were simultaneously degassed for about 30 minutes. To the solvent only flask, 0.23 g copper(I) chloride, 0.13 g copper (II) chloride and 1.1 g 2,2'-bipyridyl was placed and mixed before monomer transfer via cannula. The monomer/catalyst was subsequently sonicated and thoroughly degassed before transfer to the substrates.

Formation and photo-patterning of NPPOC-protected POEGMEMA

A 1 mM solution of 2-(2-nitrophenyl)propyl chloroformate in degassed dry dimethylformamide was generated. Amine terminated POEGMEMA substrates were immersed fully in the solution and then the flask was re-sealed under nitrogen. The minimum reaction time used was 72 h at room temperature. The selective deprotection of NPPOC-protected POEGMEMA was achieved by exposure to 325 nm wavelength laser light (He-Cd, Kimmon IK3202R-D) through a copper electron microscopy mesh grid secured with a quartz window for a dose of approximately 11.5 J cm^{-2} to achieve maximum conversion.

Surface analysis

Static contact angle of deionized water drops were measured using a Ramé-Hart model 100-00 contact angle goniometer. X-ray photoelectron spectroscopy (XPS) was carried out with a Kratos Axis Ultra DLD x-ray photoelectron spectrometer. The instrument had a monochromatic Al Kα x-ray source with an ultra-high vacuum environment. Survey and wide scans had acquisition pass energies of 160 eV and 20 eV respectively. The XPS data was analyzed using Casa XPS software (UK). All binding energies were calibrated with respect to the C 1s saturated hydrocarbon peak at 285.0 eV. Secondary mass ion spectrometry (SIMS) was conducted with an Iontof time of flight SIMS instrument, using an optimized bismuth cluster (Bi_n) primary ion source incident at 50 keV and with a 500 μm x 500 μm field of view. Ellipsometry measurements were taken on an M-2000V ellipsometer (J.A. Woollam Co., Inc.) with a white light source (370.5 to 998.7 nm) at a 70° incidence angle. The measurements were fitted with a single layer Cauchy model for a polymer brush of n = 1.5 and k = 0 with a silicon substrate (n = 3.875, k = 0.015). Multiple measurements were taken for any given sample and the brush height quoted was an average of at least three repeat measurements. A Dimension 3100 atomic force microscope with Nanoscope IIIA controller (Bruker, Santa Barbara) was used to scan images of samples in ambient conditions by tapping mode in air. Peak Force QNM images were taken using a Dimension Icon atomic force microscope with Nanoscope V controller (Bruker, Santa Barbara). The AFM tips used for tapping and Peak Force QNM were Bruker silicon TESPA (nominal stiffness 42 N m^{-1}) and silicon nitride MLCT (cantilever F, nominal stiffness 0.5 N m^{-1}) probes respectively. Force curves on freshly cleaved mica and in-built thermal noise analysis was used to estimate the spring constant of cantilevers used for Peak Force QNM. The tip radius of curvature was not calibrated and the software used default parameters.

Scheme 1. Monomers used in this work and reaction scheme for polymer chain end modification by azide reduction.

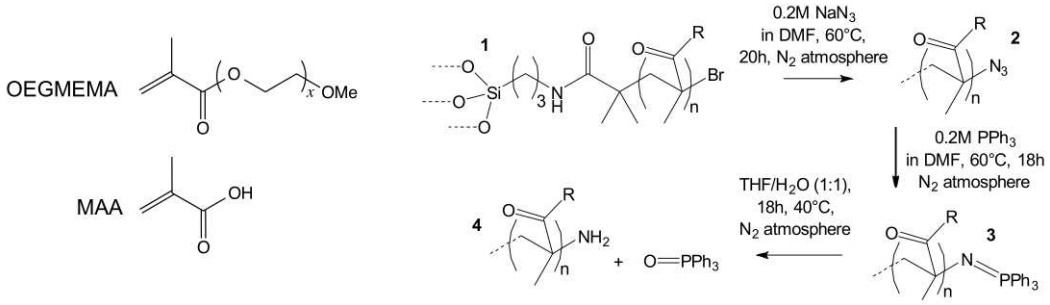

RESULTS

The processes used to fabricate and to pattern polymer brush layers are shown schematically in Figure 1 and the important chemical reactions are shown in Scheme 1. The initial poly(oligoethylene glycol methyl ether methacrylate) (POEGMEMA) brush layer was grown from an APTES surface film derivatized with bromo-initiator groups by reaction with bromoisobutyryl bromide (BIBB). Nucleophilic substitution of the alkyl bromide chain end by an azide anion with subsequent reduction and hydrolysis (Scheme 1) led to the formation of an amine chain-end-derivatized brush. The brush surface was either reactivated by treatment with BIBB and a second polymerization undertaken, or derivatized with a photocleavable moiety to allow patterned growth of a second brush (Figure 1).

Growth of poly(oligoethylene glycol methyl ether methacrylate) (POEGMEMA) and poly(methacrylic acid) (PMAA) brushes

POEGMEMA brushes were grown for various time intervals and analyzed by ellipsometry. A linear relationship was found between the brush thickness and the polymerization time, indicating that a living polymerization was occurring (Figure 2(a)). As a control, PMAA brushes were also grown from brominated silane films (although in the two-component brush patterning

scheme shown in Figure 1, the PMAA was to be grown from an initial layer of POEGMEMA). A non-linear relationship was found between the brush thickness and the polymerization time for this monomer (Figure 2(b)): the thickness increased rapidly at first, with the reaction rate reducing significantly over 90 min. This is attributed to PMAA having a very fast, non-living polymerization. However, good quality surface films were grown, despite the non-living nature of the polymerization. This is supported by the x-ray photoelectron spectroscopy (XPS) characterization of the C 1s peak with the strong ether (286.5 eV) and carboxyl (288.9 eV) peaks for POEGMEMA and PMAA in figures 2c and 2d respectively.

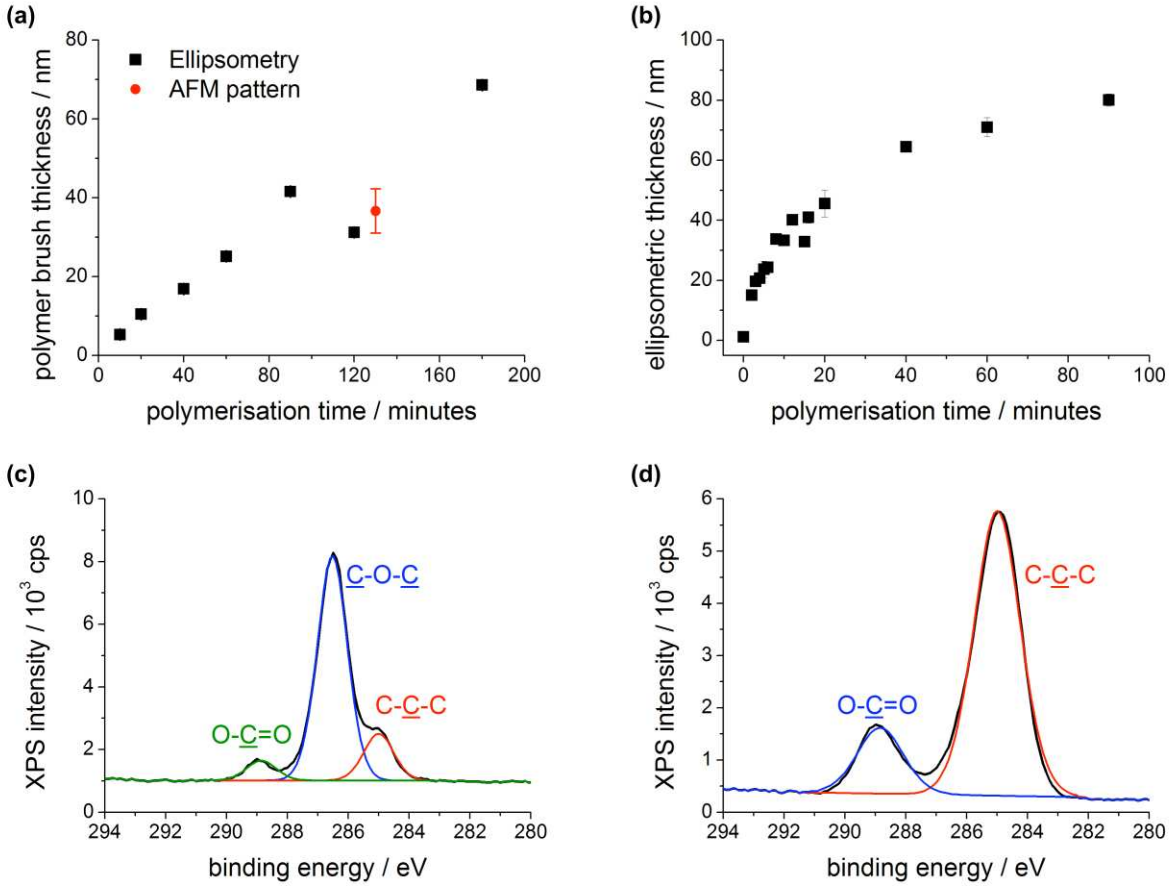

Figure 2. Polymerization kinetics of (a) poly(oligoethylene glycol methyl ether methacrylate) and (b) poly(methacrylic acid), and XPS C 1s spectra of (c) poly(oligoethylene glycol methyl ether methacrylate) brushes and (d) poly(methacrylic acid) brushes. Poly(oligoethylene glycol

methyl ether methacrylate) was synthesized using the catalyst and solvent ratios of [OEGMEMA, Cu(I)Br, bipy] = 16.7 : 1 : 2 and [H_2O, MeOH] = 1 : 4 at a solvent-monomer volume ratio of one. Poly(methacrylic acid) was synthesized using the catalyst ratios of [MAA, Cu(I)Cl, Cu(II)Cl_2, bipy] = 100 : 1 : 0.4 : 2.9 and solvent of water at a solvent-monomer ratio of three, adjusted to pH 9.

Azide substitution and reduction on brominated polymer chain ends

In a living surface-initiated ATRP reaction, the end of the growing polymer chain terminates in a bromine atom. The modification of these chain ends by reaction with sodium azide was examined. The modification involved the following steps (Scheme 1): azide nucleophilic substitution, imide formation and finally hydrolysis to yield an amine. The reaction steps were monitored by XPS. As-prepared POEGMEMA brush films were expected to contain carbon and oxygen (from the polymer chain) and bromine (at the polymer chain end). For reasonable polymerization times, the signal from the substrate and the underlying silane film would be fully attenuated because the brush thickness would be greater than the XPS sampling depth. A Br 3d peak was observed, as expected (Figure 3). After incubation of the brush layer with sodium azide, Br was undetectable within the limits of sensitivity of XPS.

A control reaction was carried out on a brominated initiator film prepared in the same way as that used to carry out ATRP (Figure S1). After treatment with sodium azide, a reduction was observed in the area of the Br 3d peak (Figure S2) and the number of components in the N 1s region was also observed to increase. For this control sample, the Br 3d signal was not reduced to zero, with a modification yield of 78 ± 1 %. This suggested it was possible that there were some residual, unmodified adsorbates after treatment with sodium azide. However, for the brush samples, the Br 3d signal reduced until it was indistinguishable from the background signal, It is

possible that the reaction between the brominated chain ends and the sodium azide was more efficient for the brush samples than for the control specimens, although the possibility cannot be excluded that a small portion chain ends in the brush remain brominated but became buried deep in the polymer layer leading to attenuation of the Br 3d signal.

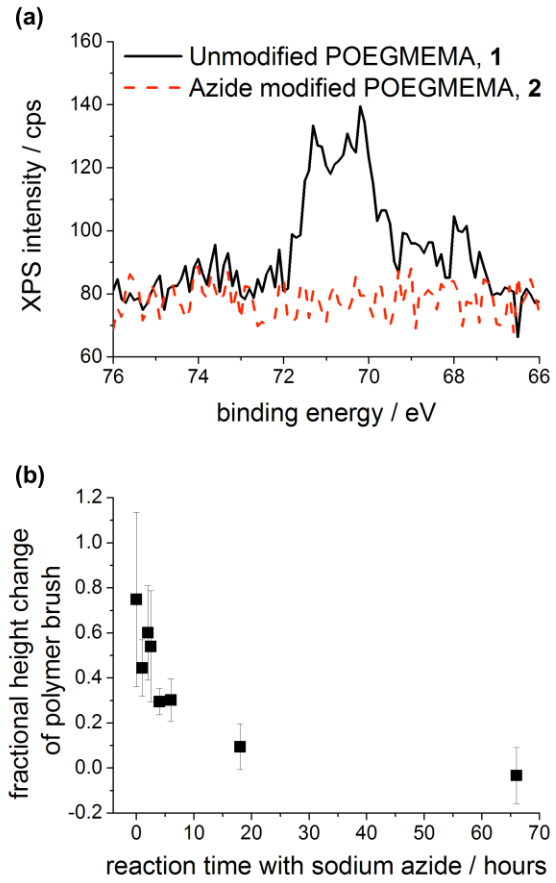

Figure 3. Characterization of azide terminated POEGMEMA brushes. (a) XPS Br 3d signal of POEGMEMA brush before and after azide substitution reaction. (b) Fractional height change from secondary brush growth on POEGMEMA (2) with azide reaction time. The immersion times were 30 and 120 min respectively for the first and second OEGMEMA polymerizations, with polymer heights measured by ellipsometry.

To further test the effectiveness of the azide end-capping reaction, ellipsometry was used to measure the extent of brush growth as a function of the reaction conditions. The time of incubation of the brushes with sodium azide was varied up to 66 h, and the polymerization reaction was carried out again. The fractional increase in the thickness of the brush layer was measured (Figure 3(b)). For short incubation times in sodium azide, a substantial increase in film thickness was measured, because the reaction was incomplete and only a small fraction of the terminal bromine atoms had been removed. However, as the incubation time increased, the increase in brush thickness was found to decrease steadily as an increasingly large fraction of the chain ends were capped. Eventually the height change reached zero, indicative of complete end-capping of the polymers. Both the 18 h and the 66 h time points have standard deviations (from four measurements on three repeats) overlapping the zero growth point suggesting that they are effective for the elimination of polymerization.

A contrasting polymer, poly(methacrylic acid) (PMAA) was grown from the initially-formed POEGMEMA layer. This necessitated re-activation of the capped chain ends in selected regions in order to allow polymerization. The impact of using a solution phase re-initiation to azide and amine terminated POEGMEMA was investigated for dry unpatterned samples by ellipsometry (Figure 4). The control sample (A) was a POEGMEMA brush film that was, after growth, not subjected to any subsequent modification (Figure 1, Scheme 1). A second control sample (B) was prepared under identical conditions to (A), but then subjected to a second polymerization with methacrylic acid as the monomer. The sample was *not* refunctionalized with initiator; rather, PMAA was grown from residual Br atoms at the ends of the polymer chains grown in the initial, living polymerization of OEGMEMA. A significant height increase of 17.8 ± 0.7 nm was observed from sample A to B. Sample (C) was treated in exactly the same way as (B), with the

exception that it was passivated with azide (Scheme 1, 2) directly after the initial polymerization of OEGMEMA. The change in brush height of 7 ± 1 nm after completion of the second polymerization reaction is substantially less than that observed for sample B, indicating extensive inhibition of polymerization by the end-capping reaction, but a small increase in height was nevertheless observed. Sample D underwent azide passivation, reduction, hydrolysis to convert the azide to an amine, and reactivation by treatment with initiator (Scheme 1, 4). Secondary PMAA brush growth of 40 ± 4 nm beyond that measured for sample C was observed for sample D. This is very much greater than was observed for the controls (A, B) and the passivated-reinitiated (C) samples.

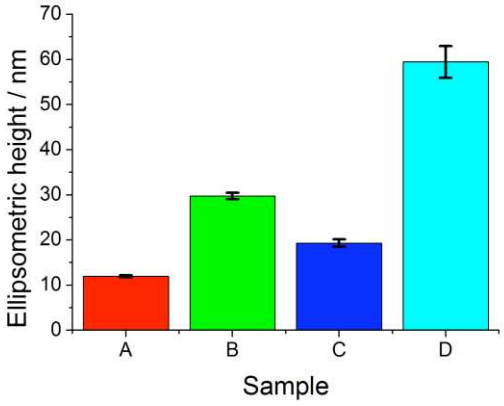

Figure 4. Comparison of methacrylic acid polymerization on uncapped (B), reinitiated azide-terminated (C), and reinitiated amine-terminated POEGMEMA (D). Sample A is POEGMEMA control (Scheme 1, 1). Sample B is POEGMEMA brush control followed by MAA polymerization. Sample C is azide passivated POEGMEMA (Scheme 1, 2) with initiation step and MAA polymerization. Sample D is amine terminated POEGMEMA (Scheme 1, 4) which undergoes initiation step and MAA polymerization. OEGMEMA and MAA polymerization times were kept constant at 30 min and 2 h respectively.

These data show that the azide end-capping reaction is highly effective as a means of terminating the ATRP process. When the surface is treated with an initiator, a small amount of derivatization of the azide occurs, but there is nevertheless a marked difference between the results for samples C and D. However, while this approach successfully yields brush copolymers, it does not provide spatial control over the location of growth of the second polymer. The feasibility of protecting the amine group, prior to the second polymerization stage, was thus explored. The goal was to enable spatially selective introduction of initiator after the conversion of the azide end-cap to an amine.

Formation of patterned polymer brush-on-brush surfaces

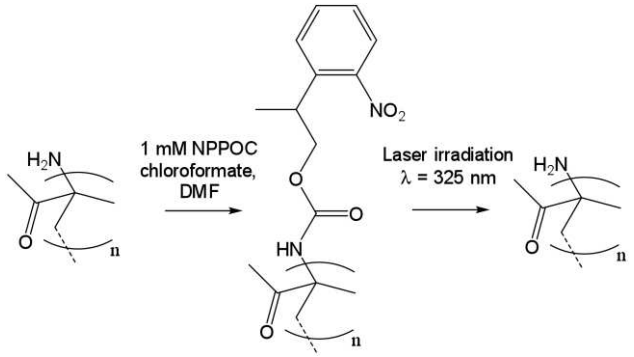

Scheme 2. Reaction scheme for coupling of amine polymer chain end with 2-(2-nitrophenyl)propyloxycarbonyl (NPPOC) chloroformate.

A nitrophenyl protecting group, the photocleavable protecting group 2-(2-nitrophenyl)propyloxycarbonyl (NPPOC), was coupled to the amine chain end. This group yields highly efficient photodeprotection on exposure to light in the near-UV region, triggering a photochemical reaction that leads to its removal to expose the protected amine[44]. In the present work, the amine-terminated POEGMEMA brush was reacted with a chloroformate precursor to form a protected amine brush (Scheme 2). Attachment of the NPPOC protecting group was

confirmed using SIMS (Figure 5(a)): a strong peak was observed at m/z 46 in the negative ion SIMS corresponding to the emission of NO_2^- ions from the nitro group.

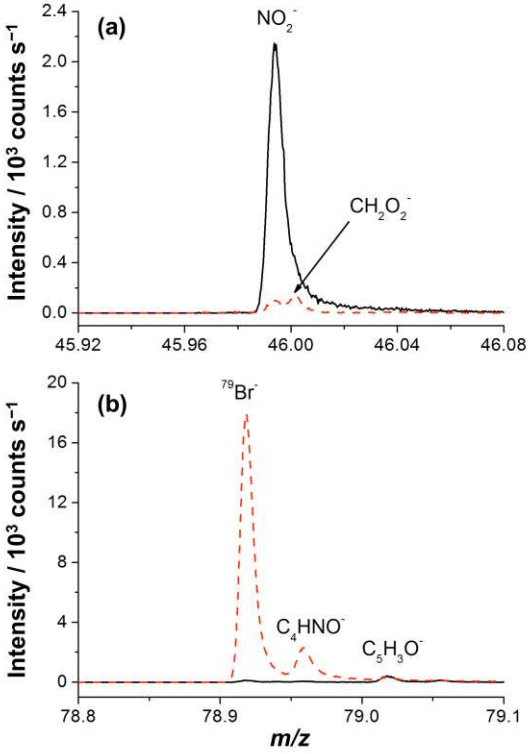

Figure 5. (a) Change in the intensity of the NO_2^- peak in the negative ion SIMS spectrum before (black line) and after (red, dashed line) photodeprotection of NPPOC-protected, amine-end-functionalized POEGMEMA brushes. (b) Change in the intensities of the $^{79}Br^-$ and C_4HNO^- peaks before (black line) and after (red, dashed line) reaction of deprotected brushes with BIBB.

NPPOC-protected amine-terminated chains were exposed to irradiation at 325 nm through a copper grid mask. In exposed regions, the protecting group was removed, yielding a substantial decrease in the area of the NO_2^- peak in the negative ion SIMS spectrum. The decrease in the peak area was substantial, suggesting almost quantitative removal of the protecting group. Deprotection of the terminal amine group facilitated its subsequent derivatization by reaction with BIBB to introduce initiators from which ATRP of methacrylic acid was used to form a

polymer brush-on-brush pattern. The attachment of the initiator was again confirmed, qualitatively, using SIMS: strong peaks were observed corresponding to Br^-. Figure 5(b) shows the strong $^{79}Br^-$ peak, together with a small adjacent peak that was attributed to a larger fragment of the BIBB-derivatized POEGMEMA, C_4HNO^-. In masked regions, the protecting group remained intact thus inhibiting attachment of the initiator.

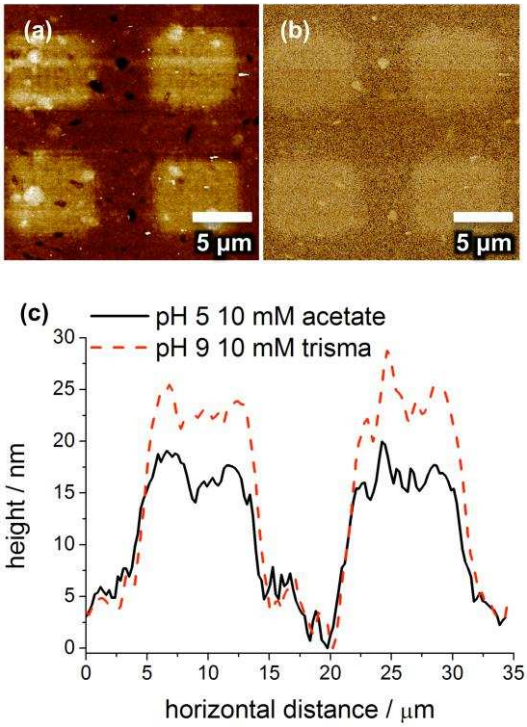

Figure 6. Tapping mode AFM images of PMAA squares grown from selectively deprotected NPPOC-terminated POEGMEMA base. (a) Height image by tapping mode AFM. Vertical scale is 16 nm. (b) Phase tapping mode AFM image in air acquired simultaneously with image in (a). The vertical scale is 70°. (c) Height cross sections from tapping mode images under 10 mM pH 5 acetate and 10 mM pH 9 tris(hydroxymethyl)aminomethane (trisma).

Patterned samples fabricated in this fashion were characterized by tapping mode AFM. Figure 6 shows data for a patterned sample which, after functionalization of the exposed regions by reaction with BIBB, was used to grow PMAA microstructures. The polymerization time used

was 2 h. Both height and phase images exhibited good contrast (Figures 6(a) and 6(b)). In exposed regions (squares in Figure 6), deprotection followed by bromination was expected to facilitate growth of PMAA brushes. A significant increase in height (ca. 7 nm. dry thickness) was observed in these regions. The phase was observed to have brighter contrast in the PMAA compared to the POEGMEMA regions, indicating a lower degree of energy dissipation. In air, the energy dissipation indicated by the phase tends to be dominated by the adhesive properties of the samples. Due to a small anionic charge on the probe tip, the electrostatic repulsion with the anionic PMAA brush led to a reduction in adhesion and hence the amount of dissipation. There were no electrostatic interactions with the POEGMEMA brush, leading to larger adhesive interactions, and therefore higher energy dissipation and the observed phase contrast.

PMAA is a stimulus-responsive polymer: at acid pH, the carboxylic acid groups are protonated and thus non-ionic. However, under basic conditions, the carboxylic acid groups become dissociated, leading to repulsive electrostatic interactions between anionic carboxylate groups and hence swelling of the brush. Line sections were taken through tapping mode height images of patterned samples to examine whether this stimulus-responsiveness was observed for patterned brushes. Figure 6(c) shows data for a single sample, acquired at pH 5 and 9. It can be seen that there was a significant difference between the heights of the PMAA features at the two pH values. In basic conditions, where the carboxylic acid groups are dissociated, the brush was ca. 6 nm (or 35%) taller than at pH 5, when the polymer was non-ionic. This increase in height reflects the swelling induced by electrostatic repulsions between PMAA chains in the exposed, square regions of the sample, confirming that the stimulus-responsive character of the polymer is retained in the patterned samples.

Peak Force Quantitative Nanomechanical (PF-QNM) is a relatively new imaging mode that allows the extraction of height and mechanical information about the sample in a similar way to force volume measurements, but with significantly shorter acquisition times. The cantilever undergoes high frequency (1 or 2 kHz) force-distance ramps. From each force-distance curve, the mechanical properties can be calculated such as tip-surface adhesion and surface stiffness. Picas and co-authors used Peak Force QNM for the analysis of supported lipid bilayers on mica[45].

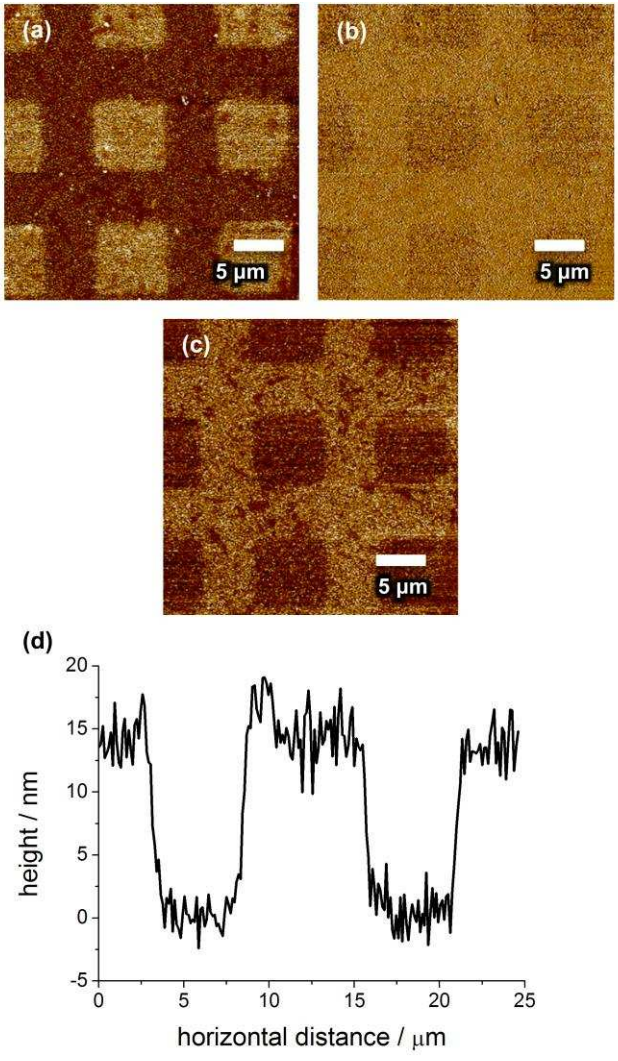

Figure 7. Peak Force QNM images in air of PMAA squares grown from selectively deprotected NPPOC-terminated POEGMEMA base. (a) Height image from Peak Force QNM. Vertical scale

is 70 nm. (b) Elastic fitting parameter image from Peak Force QNM. Vertical scale is in arbitrary units. (c) Adhesion force image from Peak Force QNM. Vertical scale is 11 nN. (d) Cross section of Peak Force QNM height image in image A. Peak Force QNM vertical scales show relative differences and not absolute values. Scale bar represents 5 μm.

PF-QNM was used to investigate the patterned samples. Figure 7 shows height, stiffness and adhesion differences between the protected and deprotected areas after methacrylic acid polymerization on a dry sample. A line section through the height image (Figure 7(a)) yields a height difference of 14 ± 2 nm between the PMAA features (squares) and the surrounding POEGMEMA. This thickness is less than the 40 nm growth measured by ellipsometry after refunctionalization of amine terminated POEGMEMA with initator and growth of PMAA under similar conditions (Figure 4, sample B). Likely the AFM data slightly under-estimate the thickness of the brush layer here. However, the data suggest that polymer chain density in the patterned regions of the two-component structures is less than 50% of the chain density in the underlying POEGMEMA layer. Given that the density of chain ends at the surface of the POEGMEMA layer is significantly less than the density of Br at the APTES film surface after treatment with BIBB this is perhaps not surprising. Critically, however, the polymer chain density in the PMAA layer is high enough for the brushes to exhibit the characteristic pH-responsive behavior (Figure 6).

Using a routine in the instrument software, a “local elastic modulus”, which has been labeled as an elastic fitting parameter, was determined from the peak force QNM data. While this quantity is related to the stiffness of the surface, it cannot strictly be described as an elastic modulus because of the use of default parameters in the fitting routine, the assumption of Derjaguin-Muller-Toporov (DMT) mechanics (likely an approximation) and the unknown

impact of higher data collection rate on higher modes of the cantilever. Nevertheless, qualitatively speaking, the data in Figure 7(b) indicate that the POEGMEMA regions are stiffer than the PMAA regions. This is consistent with expectation, given that the efficiency of reactivation of chain ends in the patterned areas (square) is likely less than 100%, which would yield a lower density of polymer chain growth in the second polymerization than in the first.

The adhesion map (Figure 7(c)) exhibited lower contrast over the PMAA regions than over the POEGMEMA regions. If the polymer density in the PMAA layer is lower than that in the POEGMEMA regions, leading to a reduced elastic modulus, it might be expected that the contact area would be increased which would, in turn, lead to an increase in the work of adhesion. However, the silica surface of the probe and the PMAA have similar pKa values, and at around neutral pH, both are expected to carry a small net negative charge. This electrostatic repulsion probably accounts for the reduced adhesion over the PMAA regions.

Secondary ion mass spectrometry (SIMS) is a powerful tool for the characterization of patterned materials, because it provides a fingerprinting capability combined with high spatial resolution. SIMS spectra of POEGMEMA and PMAA were compared. Homopolymer SIMS displayed characteristic fragments for identification. Characteristic fragments from POEGMEMA brushes (Figures S4 and S5) are related to the polyethylene glycol side group, such as ions at m/z 43 and 59 in the negative and positive ion spectra, identified as CH_2CHO^- and $CH_3OCH_2CH_2^+$ respectively. PMAA spectra (Figures S6 and S7) exhibited fewer distinctive ions that were also absent from the spectra of POEGMEMA brushes (POEGMEMA being effectively derivatized PMAA). However, characteristic peaks were observed corresponding to a monomer anion at m/z 85 and double acid monomer fragments, such as the cation found at m/z 157.

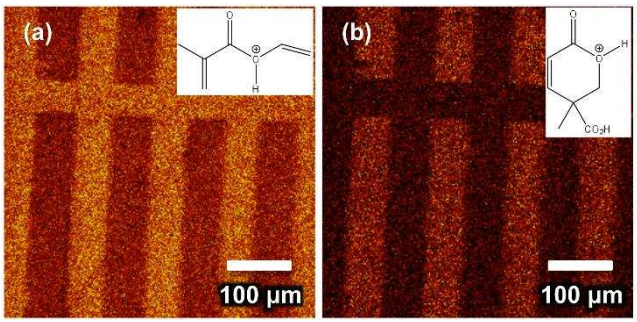

Figure 8. Secondary ion mass spectrometry images of PMAA grown on selectively deprotected POEGMEMA. The images were acquired by mapping the intensities of ions with m/z ratios of (a) 113.08 and (b) 157.08. The inset in each case shows the likely structure of the fragment whose intensity is mapped.

Retrospective chemical imaging was carried out, by collecting complete SIMS spectra from every pixel in the imaged area (256 × 256 pixels). For the SIMS measurements, a Sjostrand grid consisting of bars of width 150 and 75 µm was used as the mask during photopatterning. Analysis of the spectra for a patterned brush structure provided chemical support for the presence of two different polymers. Inverse patterns formed by mapping the intensities of ions specific to the individual polymers were observed in both negative and positive spectra. Images of characteristic ions (Figure 8) displayed well-defined chemically distinct regions, reflected in the different spatial distributions of the characteristic ions. For brush-on-brush samples, ions with m/z greater than 200 observed for POEGMEMA homopolymers were not found in brush-on-brush samples over the entire imaged region.

Cationized species were observed from PMAA regions, that yielded peaks separated by m/z 2, the difference in mass between the two copper isotopes. Positive ion spectra of PMAA homopolymers yielded peaks at m/z 63 and 65, corresponding to the elemental ions formed from the two copper isotopes. It was not expected to find copper in the final polymer. However, due to

the anionic polyelectrolyte nature of PMAA, copper cations from the catalyst solution were likely associated to the charged side chains. Copper was detectable by XPS (≤ 0.13%), indicating that it was present at low concentrations, but the superior sensitivity of SIMS enabled the distribution of copper at the surface to be mapped. Figure 9 shows images formed by mapping the intensities of two copper cationized fragments. In these images, the pattern of dark bars corresponds to the POEGMEMA regions that were masked during the patterning step; the bright contrast thus arises from the regions that were deprotected and from which PMAA was grown.

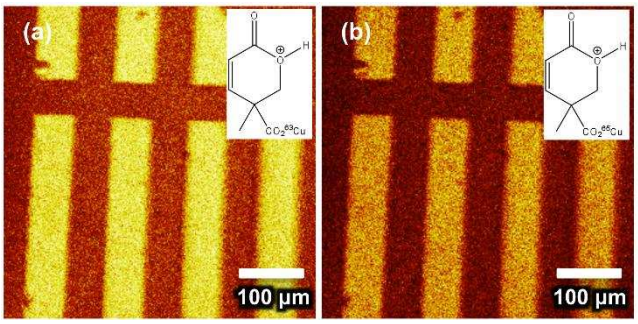

Figure 9. SIMS images of PMAA grown on selectively deprotected NPPOC-POEGMEMA. The images were acquired by mapping the intensities of ions with m/z ratios of (a) 219 and (b) 221, corresponding to the same molecular fragment but attached to, respectively, ^{63}Cu and ^{65}Cu. The inset in each case shows the likely structure of the fragment whose intensity is mapped.

DISCUSSION

The patterned brush-on-brush surfaces had significant chemical contrast that enabled visible differences to be observed by SIMS imaging, tapping mode phase imaging and Peak Force QNM adhesion force mapping. Hence a substantial amount of chemical identity remained, despite the potential for additional growth from inert regions. The presence of copper ions in the SIMS data (Figure 9) was a concern for use in biological applications and therefore immersion in a chelating agent is required in future use.

The adhesion force from Peak Force QNM was shown to be higher for POEGMEMA and lower for PMAA regions (Figure 7). This is because PMAA is an anionic polymer which exerts a repulsive force on an AFM probe with surface hydroxyl groups, while the POEGMEMA has longer side chains and hence greater effective surface area for adhesive interactions to the probe tip.

Polymer chains grafted to a surface at grafting densities below the threshold value retain a random walk conformation on the surface, which is termed a mushroom. Due to the large number of surface reactions at the chain end, the possibility of chain end radical termination during the first polymerization and the high probability of incomplete reactions at surfaces, it was expected that the grafting density for the second polymer would be less than the first polymer grown from the silane film. Hence the second polymer may have been in the mushroom regime of grafted polymer chains. The elastic fitting parameter channel of Peak Force QNM indicated that PMAA was more deformable than the surrounding POEGMEMA, which is consistent with the lower grafting density of the mushroom regime being less able to resist AFM tip penetration than the higher grafting density POEGMEMA regions.

Despite the loss of the bromine XPS signal (Figure 3a), the ellipsometry data after repeated polymerization following azide capping showed that a non-negligible amount of growth was present at the inert polymer surfaces (Figure 4). The observation of higher mass PMAA and not higher mass POEGMEMA ions from brush-on-brush samples compared to homopolymer SIMS spectra supports this conclusion, as POEGMEMA would be found lower in the sampling depth and only lower mass fragments may penetrate the top layer and be detected.

This additional growth was also present when preformed silane initiator was used (data not shown), ruling out additional initiation of unreacted amine surface silane groups. One possible

reason for the additional growth is that the azide modification was incomplete on polymer chain ends, similar to a silane surface (Figure S2), or submerged bromide chain ends of polymer being prevented from visiting the surface and being detected. Alternatively, the use of water in the polymerization solution may lead to some chain ends being converted to hydroxyl groups during the active radical state of the polymerization. Hydroxyl sites have been shown to react with acid bromide initiators[46, 47], hence upon immersion in initiator solution new chain end initiator sites with ester linkages were formed.

However, significant PMAA growth of the amine modified chain ends, as compared to azide capped chains, provided indirect evidence of successful azide reduction to amine (Figure 3). This was further evidenced indirectly by the successful patterning of a second brush after photocleavable protecting group was added to amine chain end polymer, synthesized by azide reduction (Figure 6 to 9). Indirect evidence was required for the chain end modification as it was insensitive to the available surface analysis techniques, such as XPS and SIMS, due to the very low ratio of chain end to polymer within the sampling depths. This is, to best of the authors' knowledge, the first report of azide reduction to 'grafted from' polymer chain ends by a chemical methodology.

CONCLUSIONS

A two polymer brush-on-brush patterning method using chemical azide reduction and lithography of a photocleavable protecting group has been successfully shown to generate topographic and chemical contrast. The two polymers were chemically distinguishable by SIMS and AFM methods, despite incomplete prevention of polymerization from alternative sites. Tapping mode and Peak Force QNM AFM analysis displayed height, adhesion and stiffness contrast for the patterned two layer brush. The low applied force Peak Force QNM reported a 14

nm height difference change of PMAA on POEGMEMA. The patterned PMAA was found to retain its pH-responsiveness. Characteristic ions from secondary ion mass spectrometry (SIMS) for the two polymers allowed contrast to be generated. POEGMEMA was identified by mass ions from oligoethylene glycol side chain fragmentation. PMAA had multiple monomer fragments of either organic (m/z of 157) or mixed organic-associated copper composition (m/z of 219 and 221). Amine terminated polymer brushes may be applied to protein immobilization due to the wide variety of possible coupling methodologies, while photo-patterned brush-on-brush structures allow topographic, chemically varied features to be formed by direct patterning techniques.

Supporting Information Available: data for the modification of a model surface, APTES, is provided in the supporting information. This includes a reaction scheme, XPS Br 3d envelope comparison before and after azide passivation, and static water contact angle data each reaction step. Also included are the negative and positive secondary ion mass spectra for the homopolymer brushes POEGMEMA and PMAA. This material is available free of charge via the Internet at http://pubs.acs.org.

AUTHOR INFORMATION

*Corresponding Authors. E-mail addresses: Graham.Leggett@sheffield.ac.uk; Jamie.Hobbs@sheffield.ac.uk.

†Present Address: Department of Physics, University of Warwick, Gibbet Hill Road, Coventry CV4 7AL.

ACKNOWLEDGMENT

The authors are grateful to EPSRC (Grant EP/I012060/1) for financial support and to BBSRC (Grant BB/L014904/1) for purchase of the Bruker Icon.

ABBREVIATIONS

POEGMEMA, poly(oligoethylene glycol methyl ether methacrylate); PMAA, poly(methacrylic acid); APTES, 3-aminopropyl triethoxysilane.

REFERENCES

1. Barbey, R.; Lavanant, L.; Paripovic, D.; Schüwer, N.; Sugnaux, C.; Tugulu, S.; Klok, H.-A. Polymer Brushes via Surface-Initiated Controlled Radical Polymerization: Synthesis, Characterization, Properties, and Applications. *Chem. Rev.* **2009,** *109*, 5437-5527.

2. Ducker, R.; Garcia, A.; Zhang, J.; Chen, T.; Zauscher, S. Polymeric and biomacromolecular brush nanostructures: progress in synthesis, patterning and characterization. *Soft Matter* **2008,** *4*, 1774.

3. Chen, M.; Briscoe, W. H.; Armes, S. P.; Klein, J. Lubrication at Physiological Pressures by Polyzwitterionic Brushes. *Science* **2009,** *323*, 1698-1701.

4. Bielecki, R.; Benetti, E.; Kumar, D.; Spencer, N. Lubrication with Oil-Compatible Polymer Brushes. *Tribol. Lett.* **2012,** *45*, 477-487.

5. de Beer, S.; Kutnyanszky, E.; Schön, P. M.; Vancso, G. J.; Müser, M. H. Solvent-induced immiscibility of polymer brushes eliminates dissipation channels. *Nat Commun* **2014,** *5,* 3781.

6. Raviv, U.; Giasson, S.; Kampf, N.; Gohy, J.-F.; Jerome, R.; Klein, J. Lubrication by charged polymers. *Nature* **2003,** *425*, 163-165.

7. Nomura, A.; Okayasu, K.; Ohno, K.; Fukuda, T.; Tsujii, Y. Lubrication Mechanism of Concentrated Polymer Brushes in Solvents: Effect of Solvent Quality and Thereby Swelling State. *Macromolecules* **2011,** *44*, 5013-5019.

8. Alang Ahmad, S.; Hucknall, A.; Chilkoti, A.; Leggett, G. J. Protein Patterning by UV-Induced Photodegradation of Poly(oligo(ethylene glycol) methacrylate) Brushes. *Langmuir* **2010,** *26*, 9937-9942.

9. Ma, H.; Li, D.; Sheng, X.; Zhao, B.; Chilkoti, A. Protein-Resistant Polymer Coatings on Silicon Oxide by Surface-Initiated Atom Transfer Radical Polymerization. *Langmuir* **2006,** *22*, 3751-3756.

10. Ma, H.; Wells, M.; Beebe Jr, T. P.; Chilkoti, A. Surface-Initiated Atom Transfer Radical Polymerization of Oligo(ethylene glycol) Methyl Methacrylate from a Mixed Self-Assembled Monolayer on Gold. *Adv. Funct. Mater.* **2006,** *16*, 640-648.

11. Hucknall, A.; Kim, D. H.; Rangarajan, S.; Hill, R. T.; Reichert, W. M.; Chilkoti, A. Simple Fabrication of Antibody Microarrays on Nonfouling Polymer Brushes with Femtomolar Sensitivity for Protein Analytes in Serum and Blood. *Adv. Mater.* **2009,** *21*, 1968-1971.

12. Zhang, Z.; Chen, S.; Chang, Y.; Jiang, S. Surface Grafted Sulfobetaine Polymers via Atom Transfer Radical Polymerization as Superlow Fouling Coatings. *J. Phys. Chem. B* **2006,** *110*, 10799-10804.

13. Schön, P.; Kutnyanszky, E.; ten Donkelaar, B.; Santonicola, M. G.; Tecim, T.; Aldred, N.; Clare, A. S.; Vancso, G. J. Probing biofouling resistant polymer brush surfaces by atomic force microscopy based force spectroscopy. *Colloids Surf. B: Biointerfaces* **2013,** *102*, 923-930.

14. Alswieleh, A. M.; Cheng, N.; Canton, I.; Ustbas, B.; Xue, X.; Ladmiral, V.; Xia, S.; Ducker, R. E.; El Zubir, O.; Cartron, M. L.; Hunter, C. N.; Leggett, G. J.; Armes, S. P. Zwitterionic Poly(amino acid methacrylate) Brushes. *J. Am. Chem. Soc.* **2014,** *136*, 9404-9413.

15. Li, W.; Liu, Q.; Liu, L. Antifouling Gold Surfaces Grafted with Aspartic Acid and Glutamic Acid Based Zwitterionic Polymer Brushes. *Langmuir* **2014,** *30*, 12619-12626.

16. Liu, Q.; Li, W.; Singh, A.; Cheng, G.; Liu, L. Two amino acid-based superlow fouling polymers: Poly(lysine methacrylamide) and poly(ornithine methacrylamide). *Acta Biomaterialia* **2014,** *10*, 2956-2964.

17. Chen, T.; Chang, D. P.; Liu, T.; Desikan, R.; Datar, R.; Thundat, T.; Berger, R.; Zauscher, S. Glucose-responsive polymer brushes for microcantilever sensing. *J. Mater. Chem.* **2010,** *20*, 3391-3395.

18. Gupta, S.; Agrawal, M.; Conrad, M.; Hutter, N. A.; Olk, P.; Simon, F.; Eng, L. M.; Stamm, M.; Jordan, R. Poly(2-(dimethylamino)ethyl methacrylate) Brushes with Incorporated Nanoparticles as a SERS Active Sensing Layer. *Adv. Funct. Mater* **2010,** *20*, 1756-1761.

19. Xu, F. J.; Li, Y. L.; Kang, E. T.; Neoh, K. G. Heparin-Coupled Poly(poly(ethylene glycol) monomethacrylate)-Si(111) Hybrids and Their Blood Compatible Surfaces. *Biomacromolecules* **2005,** *6*, 1759-1768.

20. Ma, H.; Hyun, J.; Stiller, P.; Chilkoti, A. "Non-Fouling" Oligo(ethylene glycol)-Functionalized Polymer Brushes Synthesized by Surface-Initiated Atom Transfer Radical Polymerization. *Adv. Mater.* **2004,** *16*, 338-341.

21. Schmelmer, U.; Paul, A.; Küller, A.; Steenackers, M.; Ulman, A.; Grunze, M.; Gölzhäuser, A.; Jordan, R. Nanostructured Polymer Brushes. *Small* **2007,** *3*, 459–465.

22. Steenackers, M.; Küller, A.; Ballav, N.; Zharnikov, M.; Grunze, M.; Jordan, R. Morphology Control of Structured Polymer Brushes. *Small* **2007,** *3*, 1764-1773.

23. Kaholek, M.; Lee, W.-K.; LaMattina, B.; Caster, K. C.; Zauscher, S. Fabrication of Stimulus-Responsive Nanopatterned Polymer Brushes by Scanning-Probe Lithography. *Nano Lett.* **2004,** *4*, 373-376.

24. Brault, N. D.; Sundaram, H. S.; Huang, C.-J.; Li, Y.; Yu, Q.; Jiang, S. Two-Layer Architecture Using Atom Transfer Radical Polymerization for Enhanced Sensing and Detection in Complex Media. *Biomacromolecules* **2012,** *13*, 4049-4056.

25. Zhou, F.; Zheng, Z.; Yu, B.; Liu, W.; Huck, W. T. S. Multicomponent Polymer Brushes. *J. Am. Chem. Soc.* **2006,** *128*, 16253-16258.

26. Zhou, F.; Jiang, L.; Liu, W.; Xue, Q. Fabrication of Chemically Tethered Binary Polymer-Brush Pattern through Two-Step Surface-Initiated Atomic-Transfer Radical Polymerization. *Macromol. Rapid Comm.* **2004,** *25*, 1979-1983.

27. Wei, Q.; Yu, B.; Wang, X.; Zhou, F. Stratified Polymer Brushes from Microcontact Printing of Polydopamine Initiator on Polymer Brush Surfaces. *Macromol. Rapid Comm.* **2014,** *35*, 1046-1054.

28. Sha, J.; Lippmann, E. S.; McNulty, J.; Ma, Y.; Ashton, R. S. Sequential Nucleophilic Substitutions Permit Orthogonal Click Functionalization of Multicomponent PEG Brushes. *Biomacromolecules* **2013,** *14*, 3294-3303.

29. Liu, Y.; Klep, V.; Luzinov, I. To Patterned Binary Polymer Brushes via Capillary Force Lithography and Surface-Initiated Polymerization. *J. Am. Chem. Soc.* **2006,** *128*, 8106-8107.

30. Konradi, R.; Rühe, J. Fabrication of Chemically Microstructured Polymer Brushes. *Langmuir* **2006,** *22*, 8571-8575.

31. Foster, E. L.; Tria, M. C. R.; Pernites, R. B.; Addison, S. J.; Advincula, R. C. Patterned polymer brushes via electrodeposited ATRP, ROMP, and RAFT initiators on colloidal template arrays. *Soft Matter* **2012,** *8*, 353-359.

32. Tria, M. C. R.; Advincula, R. C. Electropatterning of Binary Polymer Brushes by Surface-initiated RAFT and ATRP. *Macromol. Rapid Comm.* **2011,** *32* , 966-971.

33. Xu, F. J.; Song, Y.; Cheng, Z. P.; Zhu, X. L.; Zhu, C. X.; Kang, E. T.; Neoh, K. G. Controlled Micropatterning of a Si(100) Surface by Combined Nitroxide-Mediated and Atom Transfer Radical Polymerizations. *Macromolecules* **2005,** *38*, 6254-6258.

34. Fors, B. P.; Hawker, C. J. Control of a Living Radical Polymerization of Methacrylates by Light. *Angew. Chem. Int. Ed.* **2012,** *51*, 8850-8853.

35. Poelma, J. E.; Fors, B. P.; Meyers, G. F.; Kramer, J. W.; Hawker, C. J. Fabrication of Complex Three-Dimensional Polymer Brush Nanostructures through Light-Mediated Living Radical Polymerization. *Angew. Chem.* **2013,** *125*, 6982-6986.

36. Coessens, V.; Nakagawa, Y.; Matyjaszewski, K. Synthesis of azido end-functionalized polyacrylates via atom transfer radical polymerization. *Polymer Bull.* **1998,** *40*, 135-142.

37. Matyjaszewski, K.; Nakagawa, Y.; Gaynor, S. G. Synthesis of well-defined azido and amino end-functionalized polystyrene by atom transfer radical polymerization. *Macromol. Rapid Comm.* **1997,** *18*, 1057–1066.

38. Graaf, A. J. d.; Mastrobattista, E.; Nostrum, C. F. v.; Rijkers, D. T. S.; Hennink, W. E.; Vermonden, T. ATRP, subsequent azide substitution and ‘click’ chemistry: three reactions using one catalyst in one pot. *Chem. Commun.* **2011,** *47*, 6972-6974.

39. Lee, B. S.; Lee, J. K.; Kim, W.-J.; Jung, Y. H.; Sim, S. J.; Lee, J.; Choi, I. S. Surface-Initiated, Atom Transfer Radical Polymerization of Oligo(ethylene glycol) Methyl Ether Methacrylate and Subsequent Click Chemistry for Bioconjugation. *Biomacromolecules* **2007,** *8*, 744-749.

40. Li, Y.; Giesbers, M.; Gerth, M.; Zuilhof, H. Generic Top-Functionalization of Patterned Antifouling Zwitterionic Polymers on Indium Tin Oxide. *Langmuir* **2012,** *28*, 12509-12517.

41. Beier, M.; Hoheisel, J. D. Production by quantitative photolithographic synthesis of individually quality checked DNA microarrays. *Nucleic Acids Res.* **2000,** *28*, e11.

42. Hasan, A.; Stengele, K.; Giegrich, H.; Cornwell, P.; Isham, K. R.; Sachleben, R. A.; Pfleiderer, W.; Foote, R. S. Photolabile Protecting Groups for Nucleosides: Synthesis and Photodeprotection Rates. *Tetrahedron* **1997,** *53*, 4247-4264.

43. Bhushan, K. R.; DeLisi, C.; Laursen, R. A. Synthesis of photolabile 2-(2-nitrophenyl)propyloxycarbonyl protected amino acids. *Tetrahedron Lett.* **2003,** *44*, 8585-8588.

44. Alang Ahmad, S. A.; Wong, L. S.; ul-Haq, E.; Hobbs, J. K.; Leggett, G. J.; Micklefield, J. Micrometer- and Nanometer-Scale Photopatterning Using 2-Nitrophenylpropyloxycarbonyl-Protected Aminosiloxane Monolayers. *J. Am. Chem. Soc.* **2009,** *131*, 1513-1522.

45. Picas, L.; Rico, F.; Scheuring, S. Direct Measurement of the Mechanical Properties of Lipid Phases in Supported Bilayers. *Biophys. J.* **2012,** *102*, L01-L03.

46. Liu, X.; Sun, K.; Wu, Z.; Lu, J.; Song, B.; Tong, W.; Shi, X.; Chen, H. Facile Synthesis of Thermally Stable Poly(N-vinylpyrrolidone)-Modified Gold Surfaces by Surface-Initiated Atom Transfer Radical Polymerization. *Langmuir* **2012,** *28*, 9451-9459.

47. Kim, J.-B.; Bruening, M. L.; Baker, G. L. Surface-Initiated Atom Transfer Radical Polymerization on Gold at Ambient Temperature. *J. Am. Chem. Soc.* **2000,** *122*, 7616-7617.

TOC Graphic